



City Research Online

City, University of London Institutional Repository

Citation: Yazdani Nezhad, H., Auffray, A., McCarthy, C. T. & O'Higgins, R. (2015). Impact damage response of carbon fibre-reinforced aerospace composite panels. Paper presented at the 20th International Conference on Composite Materials, 19-24 Jul 2015, Copenhagen, Denmark.

This is the published version of the paper.

This version of the publication may differ from the final published version.

Permanent repository link: <https://openaccess.city.ac.uk/id/eprint/24406/>

Link to published version:

Copyright: City Research Online aims to make research outputs of City, University of London available to a wider audience. Copyright and Moral Rights remain with the author(s) and/or copyright holders. URLs from City Research Online may be freely distributed and linked to.

Reuse: Copies of full items can be used for personal research or study, educational, or not-for-profit purposes without prior permission or charge. Provided that the authors, title and full bibliographic details are credited, a hyperlink and/or URL is given for the original metadata page and the content is not changed in any way.

City Research Online:

<http://openaccess.city.ac.uk/>

publications@city.ac.uk

IMPACT DAMAGE RESPONSE OF CARBON FIBRE-REINFORCED AEROSPACE COMPOSITE PANELS

Hamed Yazdani Nezhad*, Anthony Auffray, Conor T. McCarthy, Ronan O'Higgins

Irish Centre for Composites Research, Materials and Surface Science Institute
Department of Mechanical, Aeronautical and Biomedical Engineering
University of Limerick, Ireland
Web page: <http://www.icomp.ie>

Emails: *hamed.yazdani-nezhad@ul.ie, Tel: +353 61 202253

Keywords: Fibre-reinforced composite, Delamination, Low-velocity impact, Thermoplastic, Energy dissipation

ABSTRACT

This research looks into the damage response and energy absorption behaviour of unidirectional carbon fibre-reinforced polymer (CFRP) composite panels subjected to low-velocity impact events. The response of CFRP composite materials with thermoset (TS) resin and thermoplastic (TP) PEEK polymer matrix are investigated. Evolution of impact force and absorbed energy with time during impact are presented for each TS and TP panel. Comparisons are provided between damage area obtained optically and using C-scanning technique. The investigations are based on the scanned images along with the characteristic force and absorbed energy curves for two material systems with TS and TP polymers, having similar stacking sequences, carbon volume fraction and thickness.

1. INTRODUCTION

The use of composite materials in critical aerospace structures is still limited by their relatively weak mechanical response to impact events. In addition, composite laminates subjected to low-velocity impact such as dropped tools or vehicle impact, exhibit significant internal damage and delamination, with little indication on the impact surface that such damage has occurred, generally referred to in the industry as barely visible impact damage (BVID). This has been observed by C-scanning after low-velocity drop-weight tests according to ASTM D7136 [1] carried out in several studies [2-4] which were supported by finite element simulations for uncovering the underlying damage mechanisms. Though detailed simulations have been presented by various researchers for damage response of dynamically loaded composite structures [5-10], quick accurate predictions of impact damage is still a high priority. Especially for methods that can predict the response for industrial applications, such as the ASTM standard for low-velocity impact [1] and the NASA approach for the estimation of energy dissipation during impact [11, 12].

The current study focuses on the force- and energy-time behaviour of carbon fibre-reinforced polymer (CFRP) composite panels with two aerospace grade polymer systems, a toughened thermoset (TS) resin and thermoplastic (TP) PEEK. The results of the CFRP with TS resin were taken from our previous research in [4]. All panels were impacted by low-velocity drop-weight 4.2kg impactor released from different heights representative of different impact energies. The panels were then C-scanned and damage area was captured. The force and energy data and their evolution with time were then compared and correlated to the size of damage introduced by the impactor.

It is well-known that the impact strength of TS CFRP composites can be increased by modifying the matrix with TP inclusions [13, 14]. The research in [13] suggests that the presence of TP plies in TS laminates can prevent the formation of micro-cracks possibly due to enhancement in interface properties. In this study, the low-velocity impact response of two aerospace grade CFRP material systems are investigated, one with a TP (PEEK) matrix and one with a toughened TS matrix.

The paper is divided into following main sections: Manufacturing procedure of each composite panel is briefly described in section 2, providing the geometry and the stacking configuration of the panels. Section 3 presents the basic material properties of each CFRP composite material obtained from the characterisation phase of the research. Section 4 briefly describes the impact experiments and C-scan measurement technique. Section 5 provides the existing analytical expressions used to derive absorbed energy data. The results are presented in section 6.

2. SPECIMENS MANUFACTURING AND GEOMETRY

The unidirectional CFRP composite laminates with TS and TP polymers were manufactured according to the stacking sequence provided in Table 1. The TS laminates were manufactured using unidirectional CFRP pre-pregs made of high toughness resin reinforced by carbon fibres. For laying up the TP laminates, automated tow placement (ATP) technique was used. The ATP machine is shown in Figure 1. The ATP unit uses a laser to heat the plies and consolidates them together with the aid of a roller. This unit is capable of in-situ consolidation of the TP material. Research is ongoing on the effect of ATP processing parameters on the quality and integrity of the final laminate [15, 16]. However, for this study, the ATP unit was simply used to lay-up the pre-preg in the desired stacking sequence and it was subsequently consolidated in an autoclave, according to supplier specifications shown in Figure 2.

For the case of TS laminates, each cured ply has the thickness of approximately 0.125 mm (cured using autoclave according to the specifications of the supplier). Further information for these panels is provided in [4]. Each laminate has a rectangular shape with width of 100 mm and length of 150 mm.

Layup	Stacking sequence	No. of plies	Resin type	Thick. (mm)
C	+45/90/-45/0 ₃ /-45/0/90/0/+45/0 ₃ /-45/90/+45	17	TS, TP	2.125
E	+45/90/-45/0 ₃ /+45/-45/0 ₃ /+45/90/-45/0 ₃ /-45/+45/0 ₃ /-45/90/+45	25	TS, TP	3.125

Table 1: Panel lay-ups and corresponding stacking sequences

In terms of stacking sequence, two layups were manufactured from each composite material: Layup C (relatively thin laminate) which was assessed by two impact energy levels of 10J and 20J, and Layup E (relatively thick) assessed by three impact energy levels of 10J, 20J and 40J.

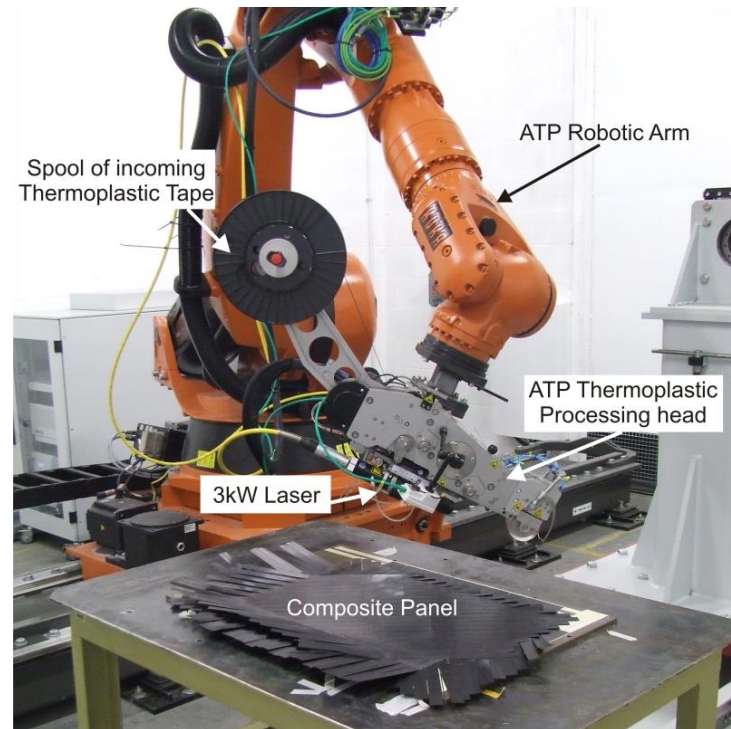


Figure 1: ATP machine installed at the University of Limerick for laying up CFRP composites

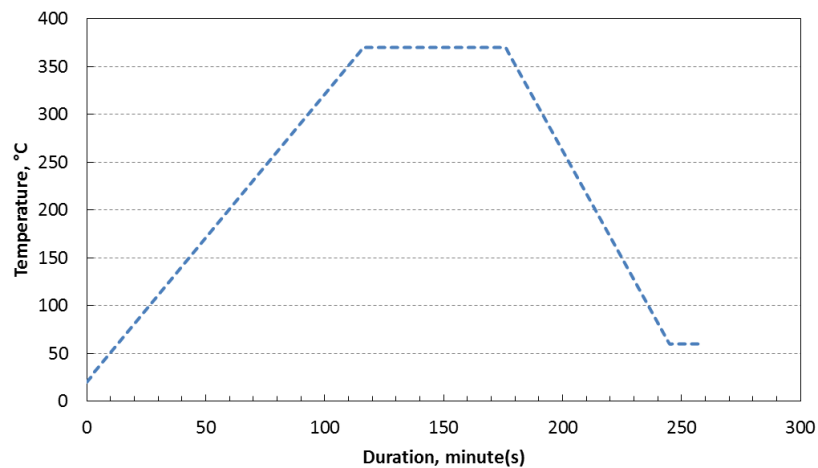


Figure 2: TP laminates' curing cycle after ATP process

3. MATERIAL CHARACTERISATION

The material characterisation was carried out for the both TS and TP laminates. Table 2 shows the linear elastic material constants of the composite plies. An obvious difference between the TS and TP material systems used in this study is the longitudinal (fibre-direction) tensile modulus which is higher for the TS system, as is tensile strength, this is primarily due to the different grade of carbon fibre used in both systems.. However, the shear strength of the TP material system is greater, as is its transverse modulus, which contributes to the out-of-plane impact behaviour of the panel.

Engineering constant	Unit	carbon fibre epoxy	Carbon fibre
		(TS) Prepreg/autoclaved	PEEK (TP) ATP/autoclaved
Longitudinal tensile modulus, E_{11}	GPa	170	135
Transverse modulus, E_{22}	GPa	8.7	9.99
Shear modulus, G_{12}	GPa	6.37	5.17
Tensile strength, S_{11}	MPa	2722	1907
Transverse strength, S_{22}	MPa	67	59
Shear strength, S_{12}	MPa	68	75
Longitudinal elongation, e_{11}	%	1.58	1.33
Transverse elongation, e_{22}	%	0.76	0.61

Table 2: Comparison of material properties of carbon fibre-reinforced TS and TP composite material systems investigated in this study

4. IMPACT TESTING AND C-SCAN MEASUREMENT

The impact tests were carried out using a drop-weight impactor test tower. The size of the samples were 100 mm × 150 mm according to [1]. The impact tester is instrumented with a load cell capable of measuring compressive forces up to 22 kN. The actual velocity at impact, v_i , was determined by measuring the time the impactor took to pass between two laser sensors, spaced 60 mm apart immediately before impact. The panel is clamped onto a rigid base using four toggle clamps with rubber tips. In the machine, the 4.2 kg impactor is raised to the desired drop height using an electric winch motor. The drop height, h , is initially estimated by $h = E_{imp}/mg$, where E_{imp} is the impact energy, m is the mass of the impactor and $g = 9.81 \text{ m/s}^2$. A pneumatic arm is employed to prevent the impactor from re-striking the test specimen if rebound occurs. Impact force as a function of time is recorded by the load cell for each impact test. The bearing and guideline friction effect was neglected in calculations.

All samples were transversely impacted out-of-plane at the centre. The C layups (17 plies) were impacted in 10J and 20J energies, and the E layups in 10J, 20J and 40J. C-scans technique was then used to capture the internal damage images of the post-impact laminates. A manual C-scanner was used, composed of a roller (GE Rotoarray) and a screen (GE Phasor XS).

5. CALCULATION OF DISSIPATION ENERGY

The energy dissipated by deformation mechanisms and damage during impact can simply be calculated by the kinematic equation according to Newton's second law of motion, provided by [1]

$$v(t) = v_i + gt - \int_0^t \frac{F(t)}{m} dt \quad (1)$$

where t is the current time during impact ($t = 0$ at the impact moment). $F(t)$ is the out-of-plane impact force introduced from the contact interaction between the impactor and the laminate, and is measured via the machine's load-cell, and $v(t)$ is the corresponding velocity of the impactor during impact. v_i , impactor velocity, can be obtained from the initial height of the impactor as described in section 4 or from the impact (kinetic) energy, E_{imp} ,

$$E_{imp} = \frac{1}{2}mv_i^2 \quad (2)$$

Friction between the impactor and the guidelines along with the machine misalignment tolerances may introduce tangential and normal forces on the impactor, which may affect the theoretical value of

v_i obtained from Eq. (2). To verify this value, v_i was measured experimentally using the laser sensors. The passing times at each sensor were recorded as t_1 and t_2 . Considering $t = t_2 - t_1$, the actual velocity was simply calculated from Eq. (1) with $F = 0$ (before impact). Comparisons between the actual and the theoretical value from Eq. (2) at different impact energies showed a negligible difference (about 0.1% overestimation by Eq. (2)).

Displacement during impact, δ , was not measured experimentally, and was obtained from

$$\delta(t) = \int_0^t v(t)dt = \delta_i + v_i t + \frac{gt^2}{2} - \int_0^t \left(\int_0^t \frac{F(t)}{m} dt \right) dt \quad (3)$$

with $\delta_i = 0$ as the initial displacement. Equation (3) was also found to provide a reasonable trend of deformation during two phases of ‘impact’ and ‘rebound’, meaning that the maximum δ , is attained at the point where the velocity becomes zero. Dissipated energy is then obtained from the conservation of energy principle, and is given by

$$E_a(t) = \frac{m(v_i^2 - v(t)^2)}{2} + mg\delta(t) \quad (4)$$

Terms $\int_0^t \frac{F(t)}{m} dt$ and $\int_0^t \left(\int_0^t \frac{F(t)}{m} dt \right) dt$ are numerically calculated as accumulative terms between the current and subsequent time steps. It is known that the total energy is absorbed when velocity becomes zero, and the deformation and damage mechanisms dissipate the initial kinetic energy introduced to the panel at the impact moment, i.e. $E_a^{max} = E_{imp}$, at $v = 0$.

Equation (4) is used to obtain the evolution of dissipated energy during impact for each laminate and energy system, from the force data obtained experimentally. The results will be discussed in section 6.

6. RESULTS AND DISCUSSION

6.1. EVOLUTION OF IMPACT FORCE AND ABSORBED ENERGY

Figure 3 shows the force-time data and energy absorption behaviour of TS and TP C-layups (relatively thin laminates) under the 10J impact energy. Three panels from each case were tested and showed consistent values and trends. Thus, only one curve is presented from each case. Both curves follow a same trend until an almost identical peak force is reached, 5100N (Figure 3(a)). The TP C-layup shows slightly higher force-time slope than the TS one. This attributes to higher transverse properties of the TP matrix prior damage initiation (see Table 2). A sudden drop then occurs in the force level of the TP C-layup that reduces the load capacity of the panel by 27%. The sudden drop attributes to the instantaneously occurring delamination damage, mostly occurring within the bottom plies. This phenomenon has been observed in other studies carried out on the TS panels (see e.g. [2] or [4]), and is believed to be the same for the TP panel examined here. This sudden drop mainly contributes to the level of absorbed energy of the TP panel after impact (so-called residual absorbed energy) as seen in Figure 3(b). This is almost zero for the TS panel with no sudden drop exhibited.

The energy is calculated based on the displacement and velocity of the impactor (Eqs. (1) to (4)) over the time increments which depend on the resolution of the data acquisition system. The effect of accumulative numerical calculation of double integrals in the above equations on the accuracy of energy estimation was primarily investigated and found negligible by changing the resolution system up to 10kHz. For example, for the case of 40J with shorter impact duration and a number of sudden drops, this effect was found more significant.

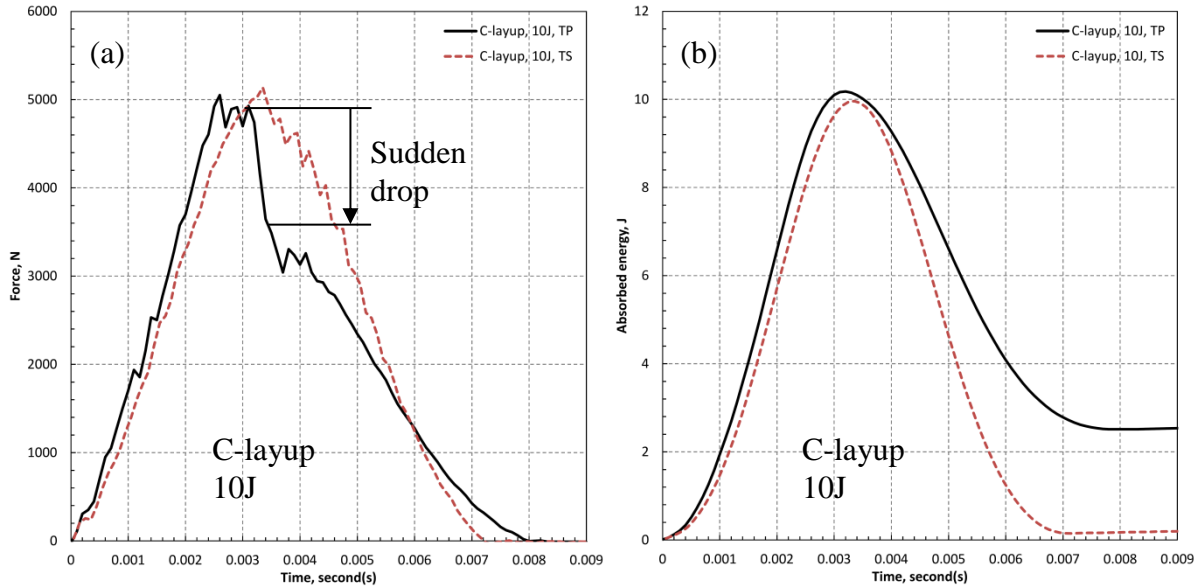


Figure 3: Comparison of TP and TS C-layups' response to 10J lateral impact energy; (a) evolution of impact force with time, and (b) absorbed energy with time

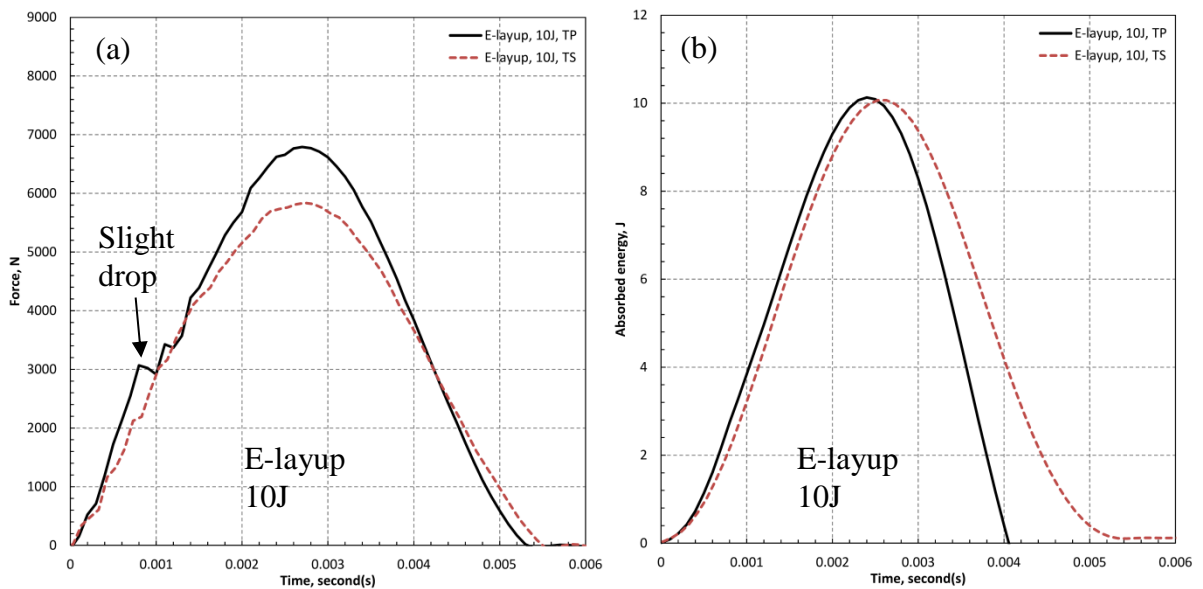


Figure 4: Comparison of TP and TS E-layups' response to 10J lateral impact energy; (a) evolution of impact force with time, and (b) absorbed energy with time

Figure 4 shows the results for the E-layups (relatively thick panel). For the TP E-layup the slope is slightly greater than the TS panel, similar to the C-layup results. The peak force reaches a higher level for the TP panel (17%). No apparent sudden drop is seen, except a slight drop at 8 milliseconds in the TP panel, which is a sign of insignificant delamination as the dominant mechanism for this phenomenon. However, this is hardly observed for the TS C- and E-layup panels which may highlight the stronger interfacial properties in the TS panel. This issue is under investigation. The residual absorbed energy of the TP and TS panels is zero (Figure 4b).

Figure 5 shows the E-layups subjected to the 20J impact energy (the results for the 20J C-layup case were not shown as they repeat the conclusions mentioned above). The sudden drop in the TP panel occurs at the peak force of 8300N, and reduces the load capacity of the panel by 22%. The intact remnant of the panel then takes up the load with a rapid rise reaching to the level of 7600N. This was

not observed in the TP C-layup case (e.g. see Figure 3). Most probably for the C-layup, the number of delaminated interfaces was sufficiently high that the remaining interfaces were not able to take up the load after the sudden drop. The TS panel with higher peak force and no apparent sudden drop exhibits a stronger response compared to the TP panel. However, the value of the residual energy of the TS panel is almost identical to the one for the TP panel. This is unexpected since the damage is less severe in the TS panel. A larger deformation is expected in the TP panel which contributes to the calculation of residual energy from Eq. (4). For the TS panel with semi-brittle behaviour with relatively small deformation/deflection, damage grows progressively with the impactor penetrating the panel at each time increment. Assuming this behaviour, damage size at each time increment is proportional to the displacement the impactor penetrates in. Therefore, damage growth can be correlated to the displacement of the impactor during the penetration phase, and therefore to the absorbed energy according to Eq. (4). However, for the TP panel exhibiting higher plasticity, the relation between these two may not simply be made through that equation. This may lead to the conclusion that Eq. (4) is only valid for the laminate-impactor systems with semi-brittle linear elastic behaviour, and becomes invalid when large deformation/plasticity is involved. Further investigation is required to clarify this.

Study of force and energy does not solely lead to a proper conclusion. C-scan technique was used to measure the introduced damage area in the panels due to impact, summarised in the following section along with the optical images.

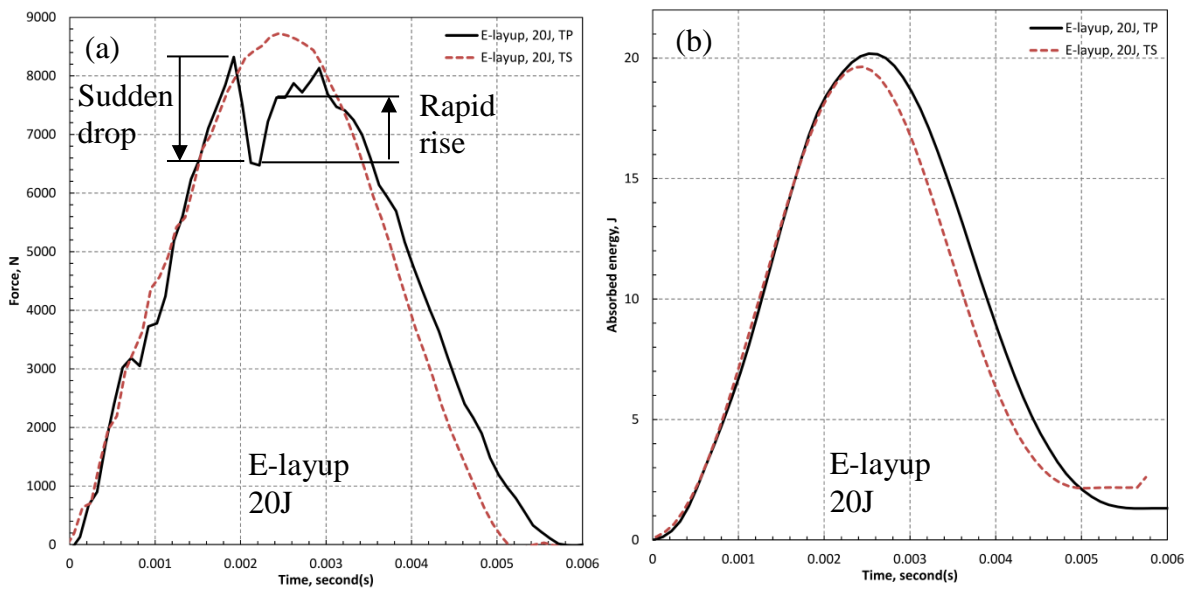


Figure 5: Comparison of TP and TS E-layups' response to 20J lateral impact energy; (a) evolution of impact force with time, and (b) absorbed energy with time

6.2. DAMAGE AREA

The optical images from the TS and TP E-layup panels are shown in Figure 6. For all cases, damage occurs more significantly at the bottom side. No significant damage was observed at the top (impacting) side except the deformation left after the penetration (Figure 7).

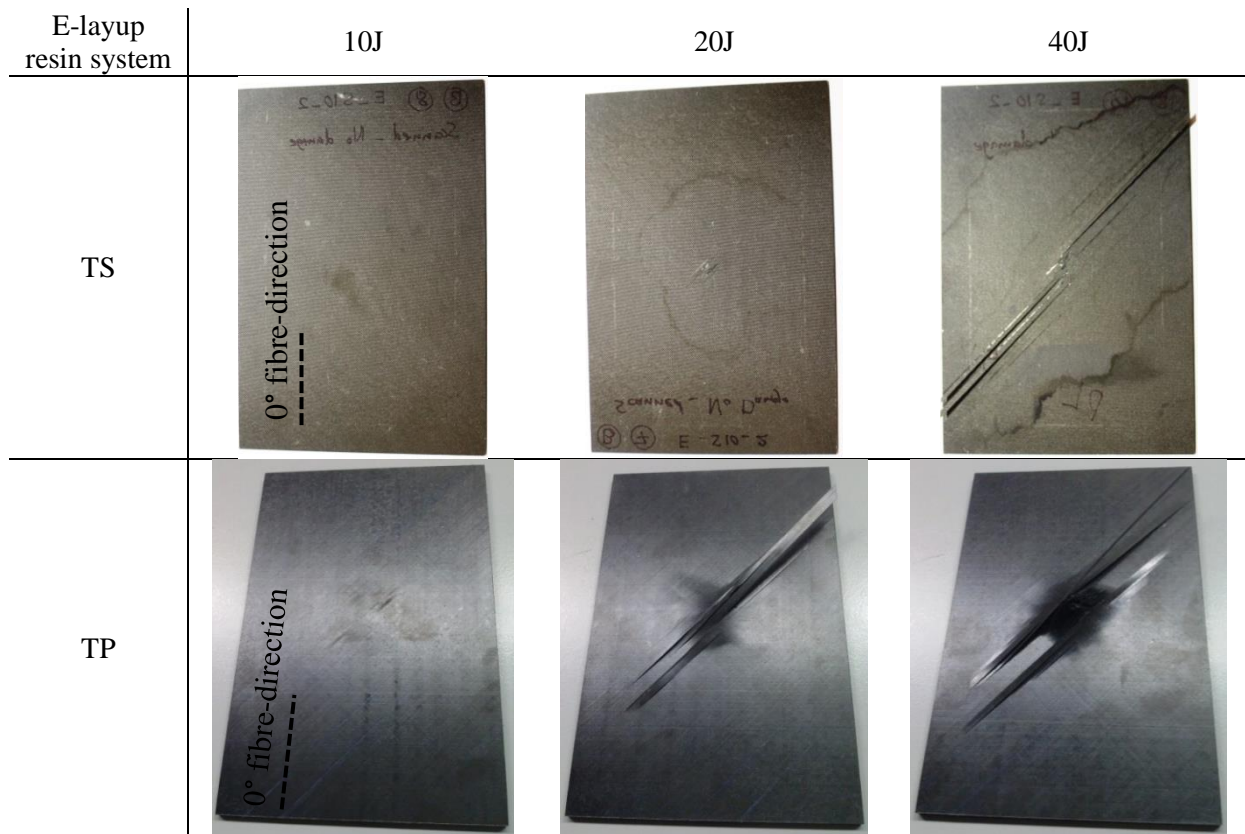


Figure 6: Evolution of damage at the bottom of E-layups (100mm × 150mm) with impact energy (10J, 20J and 40J)

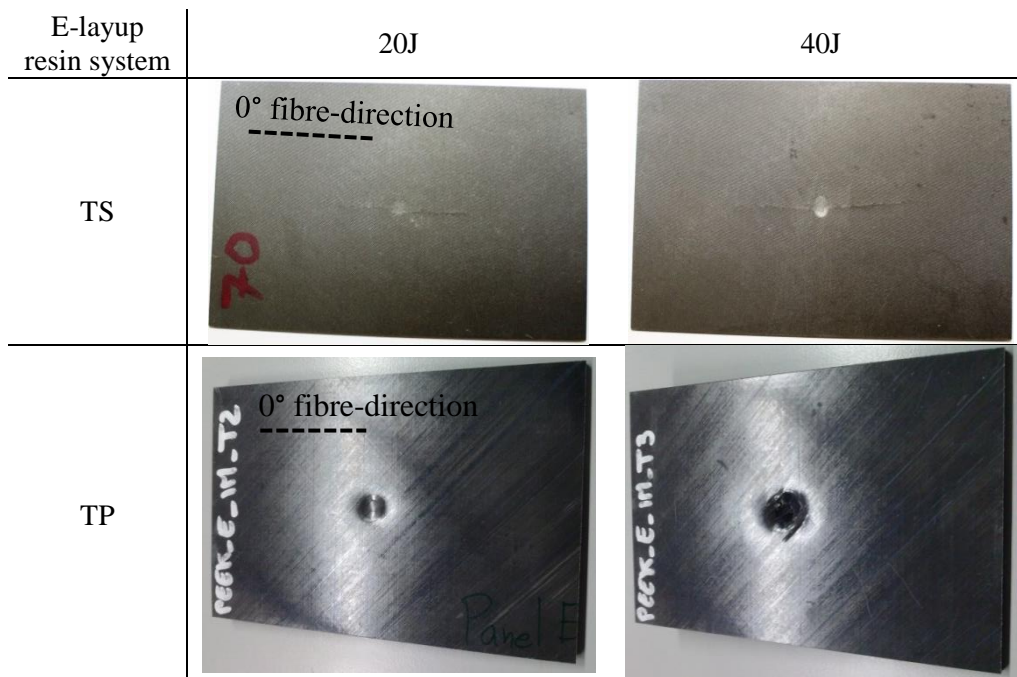


Figure 7: Evolution of damage at the top of E-layups (100mm × 150mm) with impact energy (20J and 40J)

Figure 7 shows a comparison between the impacting sides of the TS and TP panels at 20J and 40J. The impactor penetration is relatively large for the TP case due to the plastic behaviour of the

thermoplastic matrix. This is believed the reason for the absorbed energy in the TP panel to reach the same level as the TS one as shown in Figure 5.

Damage increases with increasing impact energy as seen in Figure 6 and Figure 7. However, the TS panel exhibits a greater damage resistance than the TP panel. The damage area at the bottom surface of the TS panel is not as extensive as that in the TP panel except for the 40J case.

The images from C-scan are presented in Figure 8 showing internal damage. As seen for all cases, the size of damage in the TP panel is larger than that in the TS panel. Damage in TP panel grows radially with the increasing energy keeping a semi-elliptical shape from the impact centre while in the TS panel it grows inclined with 0° and 45° angles.

It may be noted that the C-scan images show a combination of in-plane damage and delamination, and thus separating interply delamination from in-plane damage is not simple. Our previous research has shown that the energy is predominantly absorbed by delamination mechanisms in the TS panel (larger than 60% of the total energy) [4]. However, as discussed in section 6.1 on the results of Figure 5, the dominant mechanism in terms of energy absorption behaviour might be different in TP panels (if Eq. (4) is assumed reliable). Further investigations are required along with the numerical analysis for understanding the underlying mechanisms involved in the impact damage response of the TP CFRP laminates.

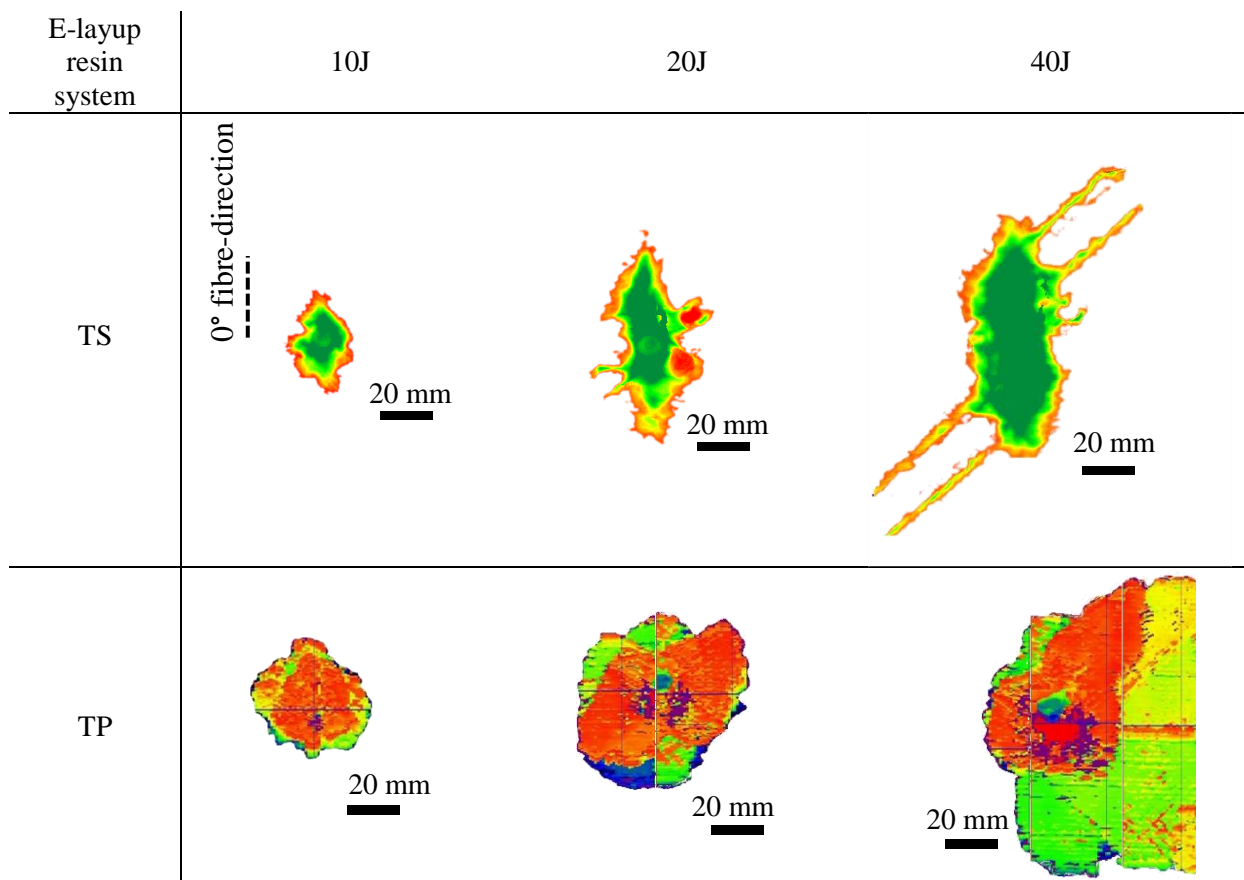


Figure 8: Evolution of damage in E-layups (100mm × 150mm) with impact energy (10J, 20J and 40J) measured by C-scanning technique

7. CONCLUSIONS

The low-velocity impact response of CFRP composite laminates with two polymer systems (thermoset toughened epoxy and thermoplastic PEEK) were studied in this research. The focus was

mainly on the comparison of the impact characteristic curves obtained from drop-weight impact tests and C-scans to visualise impact damage within the panels. The study showed that the toughened TS epoxy material system performed slightly better than the TP PEEK material system. The peak force was almost identical for the both panels. However, significant sudden drop in the load capacity of the TP panels was seen. This phenomenon was recovered with a rapid rise in load carrying level in the thick panel (E-layup). The extent and shape of damage were also studied. It was seen that in the TS panels, damage is essentially trapped and allowed to extend mostly in 0° and 45° directions with slight radial growth as opposed to the extensive damage growth in the TP panels. The estimation of absorbed energy via Eq. (4) was found inaccurate for the TP panels and thus further investigation is suggested. The study shows that new toughened fibre-reinforced TS epoxy systems perform as well, if not better, under out of plane impact loading as fibre-reinforced PEEK material systems.

ACKNOWLEDGEMENTS

The funding for the project has been provided by various grants. The authors would like to acknowledge Enterprise Ireland (grant CF/2013/3012B) for the project of Design of Optimised Composites for Impact Applications (OPTCOM) and Science Foundation Ireland (grant 13/IA/1833) for the project of Fastener-less Joining Technologies for High Performance Hybrid Composites-Metal Structure (FALCOM). The thermoset layups were manufactured and tested in a previous research. The research leading to these results has received funding from the European Community's Seventh Framework Programme FP7/2007-2013 under grant agreement n°213371 (MAAXIMUS, www.maaximus.eu).

8. REFERENCES

1. *ASTM D7136 / D7136M - 07 Standard Test Method for Measuring the Damage Resistance of a Fiber-Reinforced Polymer Matrix Composite to a Drop-Weight Impact Event*. 2003.
2. Gonzalez, E.V., P. Maimi, P.P. Camanho, A. Turon, and J.A. Mayugo, *Simulation of drop-weight impact and compression after impact tests on composite laminates*. Composite Structures, 2012. **94**(11): p. 3364-3378.
3. Shi, Y., T. Swait, and C. Soutis, *Modelling damage evolution in composite laminates subjected to low velocity impact*. Composite Structures, 2012. **94**(9): p. 2902-2913.
4. Nezhad, H.Y., F. Merwick, R.M. Frizzell, and C.T. McCarthy, *Numerical analysis of low-velocity rigid-body impact response of composite panels*. International Journal of Crashworthiness, 2015. **20**(1): p. 27-43.
5. Johnson, A.F., A.K. Pickett, and P. Rozycki, *Computational methods for predicting impact damage in composite structures*. Composites Science and Technology, 2001. **61**(15): p. 2183-2192.
6. Johnson, A.F. and M. Holzapfel, *Influence of delamination on impact damage in composite structures*. Composites Science and Technology, 2006. **66**(6): p. 807-815.
7. Bouvet, C., B. Castanie, M. Bizeul, and J.J. Barrau, *Low velocity impact modelling in laminate composite panels with discrete interface elements*. International Journal of Solids and Structures, 2009. **46**(14-15): p. 2809-2821.
8. Lopes, C.S., P.P. Camanho, Z. Gurdal, P. Maimi, and E.V. Gonzalez, *Low-velocity impact damage on dispersed stacking sequence laminates. Part II: Numerical simulations*. Composites Science and Technology, 2009. **69**(7-8): p. 937-947.

9. Zhou, Y.H., H. Yazdani-Nezhad, M.A. McCarthy, X.P. Wan, and C. McCarthy, *A study of intra-laminar damage in double-lap, multi-bolt, composite joints with variable clearance using continuum damage mechanics*. *Composite Structures*, 2014. **116**: p. 441-452.
10. Yazdani Nezhad, H., B. Egan, F. Merwick, and C.T. McCarthy, *Bearing Damage Characteristics of Quasi-statically Loaded Fibre-reinforced Composite Bolted Joints*. *Composite Structures*, 2015.
11. Chamis, C.C. and J.H. Sinclair, *NASA TM-83594: Impact Resistance of Fiber Composites: Energy Absorbing Mechanisms and Environmental Effects*. 1996: NASA Lewis Research Center, Cleveland, Ohio.
12. Shivakumar, K.N., W. Elber, and W. Illg, *NASA TM-85703: Prediction of Impact Force and Duration During Low Velocity Impact on Circular Composite Laminates*. 1983, NASA Langley Research Centre, Hampton, VA.
13. He, Y.X., Q. Li, T. Kuila, N.H. Kim, T. Jiang, K.T. Lau, and J.H. Lee, *Micro-crack behavior of carbon fiber reinforced thermoplastic modified epoxy composites for cryogenic applications*. *Composites Part B-Engineering*, 2013. **44**(1): p. 533-539.
14. Bora, M.O., O. Coban, T. Sinmazcelik, I. Curgul, and V. Gunay, *On the life time prediction of repeatedly impacted thermoplastic matrix composites*. *Materials & Design*, 2009. **30**(1): p. 145-153.
15. Comer, A.J., D. Ray, W.O. Obande, D. Jones, J. Lyons, I. Rosca, R.M. O'Higgins, and M.A. McCarthy, *Mechanical characterisation of carbon fibre-PEEK manufactured by laser-assisted automated-tape-placement and autoclave*. *Composites Part a-Applied Science and Manufacturing*, 2015. **69**: p. 10-20.
16. Ray, D., A.J. Comer, J. Lyons, W. Obande, D. Jones, R.M.O. Higgins, and M.A. McCarthy, *Fracture toughness of carbon fiber/polyether ether ketone composites manufactured by autoclave and laser-assisted automated tape placement*. *Journal of Applied Polymer Science*, 2015. **132**(11): p. 10.